IEEE Photonics Journal
An IEEE Photonics Society Publication

Open Access

Optical Tweezers With Fractional Fractal Zone Plate

Volume 8, Number 5, October 2016

Shubo Cheng
Shaohua Tao
Xinyu Zhang
Wenzhuo Ma

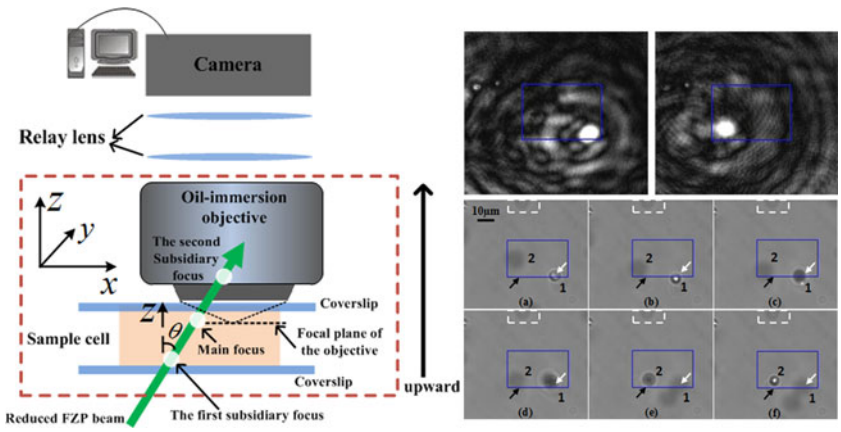

DOI: 10.1109/JPHOT.2016.2614760
1943-0655 © 2016 IEEE

Optical Tweezers With Fractional Fractal Zone Plate

Shubo Cheng,[1] Shaohua Tao,[1,2] Xinyu Zhang,[1] and Wenzhuo Ma[1]

[1]School of Physics and Electronics, Central South University, Changsha 410083, China
[2]Hunan Key Laboratory of Super Microstructure and Ultrafast Process, Central South University, Changsha 410083, China

DOI:10.1109/JPHOT.2016.2614760
1943-0655 © 2016 IEEE. Translations and content mining are permitted for academic research only. Personal use is also permitted, but republication/redistribution requires IEEE permission. See http://www.ieee.org/publications_standards/publications/rights/index.html for more information.

Manuscript received June 15, 2016; revised September 19, 2016; accepted September 27, 2016. Date of publication September 30, 2016; date of current version October 19, 2016. This work was supported by the National Natural Science Foundation of China under Grant 61178017. Corresponding author: S. H. Tao (e-mail: eshtao@csu.edu.cn).

Abstract: Free-space propagations of the optical beams generated by the fractal zone plates with fractional structural parameters [i.e., fractional fractal zone plate (FZP)] are analytically studied in this paper. The results demonstrate that the axial location of the main focus and axial distance between two neighboring foci of the fractional FZP beam can be precisely customized. Furthermore, we first demonstrate optical manipulation with the fractional FZP beam. The experimental results verified that such an FZP beam can simultaneously trap multiple particles positioned in different focal planes of the beam, owing to the multiple foci and self-reconstruction property of the FZP beam. The customized locations of trapped particles can also be realized by the fractional FZP beam, which would be useful for constructing three-dimensional optical tweezers.

Index Terms: Fractional fractal zone plate (FZP), self-reconstruction, optical tweezers.

1. Introduction

Highly focused laser beams are widely used to trap various types of particles such as transparent silica or polymer spheres, coated microspheres, and so on [1]–[3]. Conventionally, only the optical fields in the imaging plane can be controlled. Thus, the microparticles in multiple planes cannot be manipulated simultaneously. Although multiple microparticles can be trapped in 3-D space via several methods such as time-sharing, specific beam shaping algorithms, and so on [4]–[6], the subsequent propagation of the beam would be affected by the reflection, refraction, or absorption of a trapped particle.

To realize 3-D trapping of multiple particles in 3-D space, one can generate an optical beam with tailorable intensity distribution and the self-reconstruction property [7] along the propagation axis of the beam. A few beams, e.g., Bessel beams, Airy beams, and others, were found to possess the self-reconstruction property and used to trap multiple particles simultaneously [8]–[10], but positions of the trapped particles in 3-D space could not be customized owing to the diffraction properties of the beams. Although the optical beams generated by fractal zone plates (FZPs) were proved to possess the self-reconstruction property and the focal lengths of multiple foci provided by the beam can be tailored by adjusting the structural parameters of the FZP [11], [12], the axial distance between two neighboring foci of an FZP beam can only be roughly adjusted. Furthermore, a fractal structure lens named devil's lens was used in optical tweezers [13], but the focal length of the lens cannot be tailored precisely and the trappings of multiple foci have not been implemented.

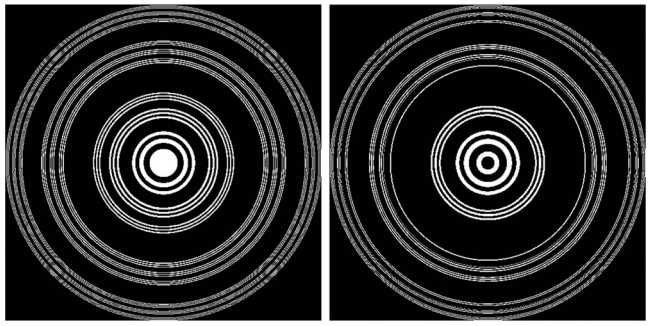

(a) (b)

Fig. 1. FZPs with (a) N = 3 and S = 3 and (b) N = 2.9 and S = 3. The bright and dark segments correspond to the transmittances of 1 and 0, respectively.

Conventionally, the number of fractal segments of an FZP is an integer [11], but the number can be fractional [12]. We name the FZP with a fractional number of fractal segments as fractional FZP. In this paper we first demonstrate the capability of the optical beams generated by the fractional FZP in constructing 3-D optical tweezers. The main focus and the second subsidiary foci of the beam will be used to separately trap and manipulate particles at different focal spots in 3-D space. Furthermore, dynamic manipulation of microparticles in optical tweezers will be implemented by changing Ns of the fractional FZPs. The unique diffraction properties such as the self-reconstruction property and customizable focal length of the fractional FZP beam are found to be privital for the implementation of the 3-D manipulation.

2. Axial Properties of the Fractional FZP

The FZPs can be constructed from conventional Fresnel zone plates in some cases [11]. Usually, one-dimensional fractal structure of the binary Cantor sets can be adopted for the construction of an FZP. The optical beam generated by an FZP was found to possess multiple foci with internal fractal properties along the optical axis [11]. Although many specified FZPs [14]–[19] have been proposed, the focal length of multiple foci provided by the FZP beam, e.g., the FZP beam with an integer of fractal segments, can be only roughly adjusted. Fig. 1(a) shows an example FZP with N = 3 and S = 3, where N and S are the numbers of fractal segments and stage, respectively [11]. In our recent investigation [12] the axial locations of multiple foci and the axial distance between two neighboring foci of a fractional FZP beam can be precisely adjusted by modifying the fractional number N. Furthermore, the fractional FZP beams are also found to possess the self-reconstruction property [12]. Fig. 1(b) shows an example fractional FZP with N = 2.9 and S = 3.

The transmittance of a single FZP comprises 0 and 1 meaning that the corresponding zone of the FZP is opaque or transparent to the incident beam [11]. The transmittance values of 0 and 1 of the FZP can be replaced with phase steps of 0 and π, respectively, for the higher diffraction efficiency of phase-only diffractive optical elements [20]. Furthermore, the focal length of the main focus of an FZP beam can be expressed by (1) [14], shown below, and it has been proved that the focal length of a fractional FZP beam can be still expressed by [12]

$$f(a, \lambda, N, S) = a^2 \cdot \left[\lambda \cdot (2N - 1)^S\right]^{-1} \tag{1}$$

where a is the radius of the FZP, λ is the wavelength of the illuminating light, N is the number of the segments forming the fractal structure, and S is the fractal stage.

A collimated laser beam with a wavelength of 532 nm was applied in the following simulations and trapping experiments. The radii of the FZPs are set as 256 $\times$ 15 μm. Propagations of the FZP beam in free space are simulated by using the angular spectrum of the plane wave method. As an example, the axial irradiance of the FZP with N = 3 and S = 3 is shown in Fig. 2(a) and

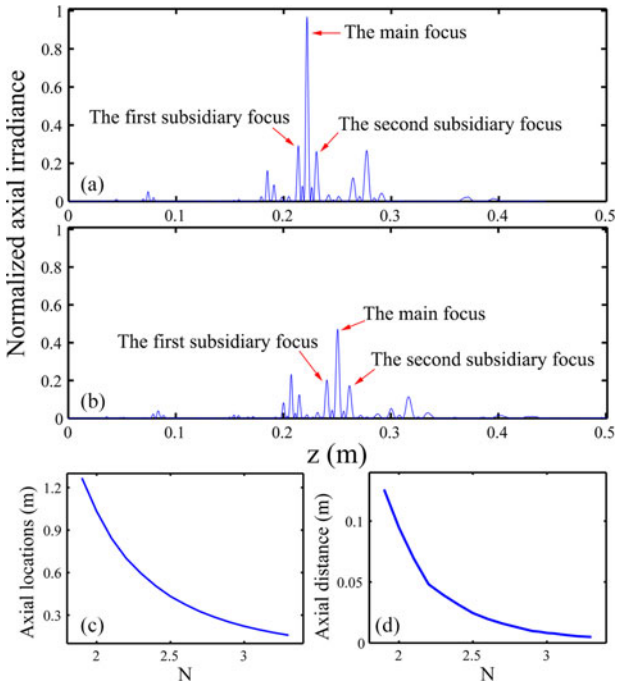

Fig. 2. Axial irradiance of the FZPs with (a) N = 3, S = 3 and (b) N = 2.9, S = 3. Plots of (c) axial location of the main focus from the SLM and (d) axial distance between the main focus and the second subsidiary focus of an FZP beam with S = 3 versus N.

the counterpart of the fractional FZP with N = 2.9 and S = 3 is shown in Fig. 2(b). The main foci in Fig. 2(a) and (b) have the calculated distances of 221.7 mm and 250.7 mm from the FZPs, respectively. The peaks around the respective main focus are marked as the first subsidiary focus and the second one, respectively. The average axial distance between two neighboring foci (i.e., the main focus and subsidiary foci) of the FZP beam with N = 3 and S = 3 is about 8.5 mm and the counterpart of the fractional FZP with N = 2.9 and S = 3 is about 10.3 mm. The plots of axial location of the main focus and axial distance between the main focus and the second subsidiary focus of an FZP beam with S = 3 versus N are shown in Fig. 2(c) and (d), respectively. Obviously, when N is changed with a fractional increment, both the axial locations and the axial spacings of the foci of the FZP beam can be more precisely controlled. Thus, microparticles can be dynamically manipulated by changing Ns of the fractional FZPs.

It is worth mentioning that although the fractional FZP beam has weaker foci than the FZP beam with an integer of N in Fig. 2(a) and (b), the fractional FZP beams can be still used to trap microparticles due to the intensity-gradient force. As the fractional FZP beams are found to have the self-reconstruction property [12], the trapped particles will not affect the subsequent propagation of the beam. This will be beneficial to stable trapping of microparticles in multiple planes. In the following multi-plane trapping experiments, we will use the FZP shown in Fig. 1(b) so that the shifts of the foci in the viewfield can be observed clearly. Considering the limited depth of the sample cell and short work distance of the objective, we will use the main focus and the second subsidiary focus shown in Fig. 2(b) to trap microparticles.

3. Optical Trapping of Microparticles With the Fractional FZP Beam

The schematic of the whole optical trapping system can be referred to [21]. A Gaussian beam emitting from an optically pumped semiconductor laser with maximum output power of 1 *W* is expanded with a beam expander and then projected onto the spatial light modulators (SLMs: BNS, XY Nematic Series, 512 × 512 pixels, phase type, pixel pitch = 15 μm). The reconstructed FZP

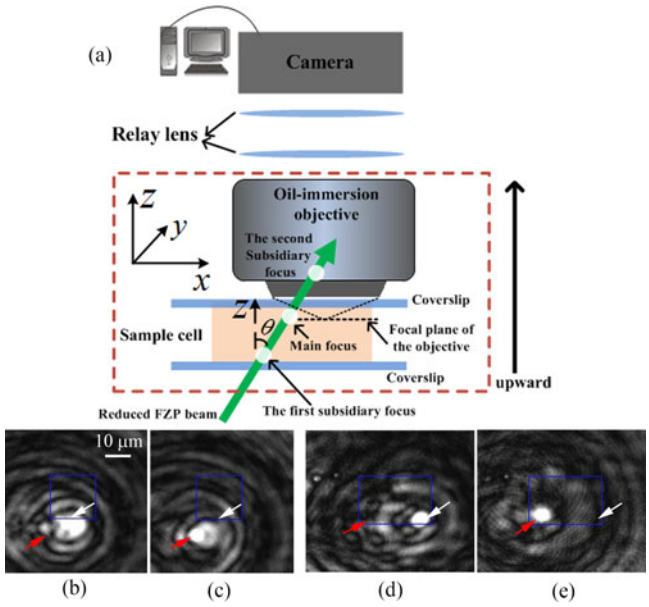

Fig. 3. (a) Schematic of the experimental setup. Captured CCD frames of intensity distributions of (b) the main focus and (c) the second subsidiary focus of the FZP beam with N = 3 and S = 3. Captured CCD frames of intensity distributions of (d) the main focus and (e) the second subsidiary focus of the fractional FZP beam with N = 2.9 and S = 3. The locations of the main focus and the second subsidiary focus are highlighted with white and red arrows, respectively.

beam from the SLM is further reduced 25 times with a telescope. The optical arrangement around the sample cell is schematically shown in Fig. 3(a), where the reduced FZP beam incidents to the sample cell at a small oblique angle. In the trapping experiments polystyrene beads with a diameter of about 5 μm were immersed in deionized water of refractive index of 1.33. The oblique incidence of the beam ray in Fig. 3(a) facilitates the observation of three-dimensional trapping of microparticles in multiple focal planes. It is worth mentioning that the relative distance between the objective and the sample cell was fixed in the trappings.

In Fig. 3(a), the main focus of the FZP beam with N = 3 and S = 3 is located at the focal plane of the objective. The observed main focus in the viewfield of the CCD camera is shown in Fig. 3(b). When the sample cell and the objective were shifted upward synchronously about 180 μm, the second subsidiary focus is just located at the focal plane of the objective and we can observe the image of the focus clearly in the viewfield of the CCD camera as is shown in Fig. 3(c). Similarly, when the fractional FZP beam with N = 2.9 and S = 3 is used in the optical tweezers system, the image of the observed main focus in the viewfield of the CCD camera is shown in Fig. 3(d). Differently, only when the sample cell and the objective were shifted upward synchronously about 360 μm, can we observe the image of the second subsidiary focus clearly in the viewfield. The image is shown in Fig. 3(e). Compared with the FZP beam with N = 3 and S = 3, the axial distance between the main focus and the second subsidiary focus of the fractional FZP with N = 2.9 and S = 3 is increased slightly. Furthermore, we can observe that the locations of the foci shift toward a fixed direction in the viewfield of the CCD camera due to oblique incidence of the FZP beam ray. Comparing Fig. 3(b) and (c) with Fig. 3(d) and (e), we find that the shifting displacement of the second subsidiary focus from the main focus of the fractional FZP with N = 2.9 and S = 3 is slightly greater than that of the FZP with N = 3 and S = 3 in the viewfield. The results are in agreement with those shown in Fig. 2(a) and (b). Thus, the axial distance between two neighboring foci of an FZP beam can be precisely adjusted by setting N as a fraction.

Optical trapping experiments were implemented with the optical beam generated by the fractional FZP shown in Fig. 1(b). In the trapping experiments, the laser power was set to 950 mW. In the beginning, the main focus of the fractional FZP beam with N = 2.9 and S = 3 was located at the

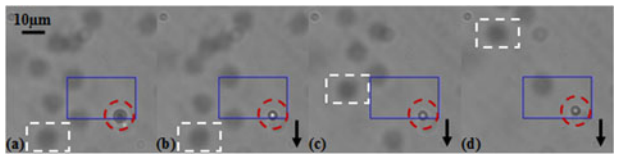

Fig. 4. (a)–(d) CCD-captured frames showing that a particle highlighted with a dashed circle is trapped by the main focus and moves horizontally with the shifting focus.

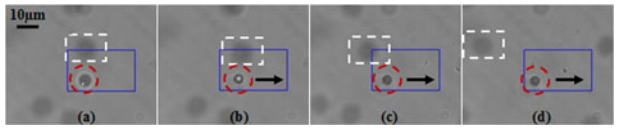

Fig. 5. (a)–(d) CCD-captured frames showing that a particle is trapped and then moves horizontally with the second subsidiary focus of the FZP beam.

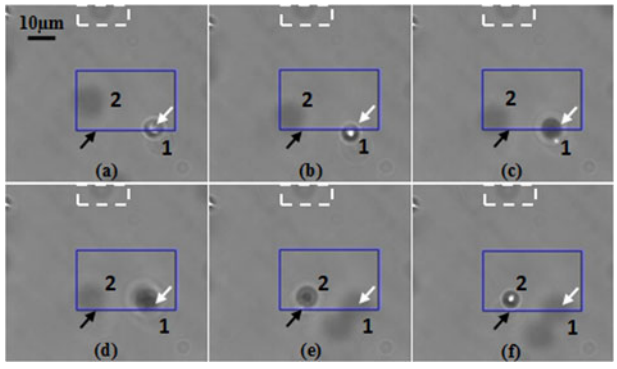

Fig. 6. Experimental demonstration of simultaneous trapping with two foci of the fractional FZP beam of N = 2.9 and S = 3. (a)–(b) Trapping of a cluster of particles marked as 1 with the main focus, (c)–(f) trapping of a particle marked as 2 with the second subsidiary focus and in the mean time trapping of the particles marked as 1 with the main focus.

focal plane of the objective in Fig. 3(a). The image of the main focus in the viewfield is shown on the right bottom of the exposure region of Fig. 3(d). A polystyrene bead was attracted toward the main focus and then trapped stably. Fig. 4(a)–(d) show the sequential CCD-captured frames demonstrating that the trapped polystyrene bead was manipulated horizontally. Then, the sample cell and the objective were shifted upward synchronously about 360 μm until the second subsidiary focus was just located at the focal plane of the objective. The image of the second subsidiary focus in the viewfield is located at the left bottom of the exposure region of Fig. 3(e). A polystyrene bead around the focus was trapped and moved. The trappings are shown in Fig. 5(a)–(d). In Figs. 4 and 5, the particle highlighted with the white dashed rectangle is the background particle and the black arrows represent the movement of the trapped particle. Hence, we can see from Figs. 4 and 5 that each of the foci, i.e., the main focus and the second subsidiary focus of the fractional FZP beam, is capable of manipulating particles stably.

In order to verify the ability of 3-D trapping of microparticles with the fractional FZP beam with N = 2.9 and S = 3, we first located the main focus of the beam at the focal plane of the objective in Fig. 3(a). It is observed that the polystyrene beads marked as 1 were trapped from Fig. 6(a) and (b), where the white and black arrows highlighted the locations of the main focus and the second subsidiary focus, respectively. Then, the sample cell and the objective in Fig. 3(a) were shifted upward synchronously and in the mean time the main focus was relatively shifted toward the bottom of the sample cell. From Fig. 6(b)–(e), we can see that the beads marked as 1 were still trapped stably and shifted downward with the main focus. Thus, the image of the trapped beads 1 changed dim gradually in the viewfield of the CCD camera. The sample cell and the objective were

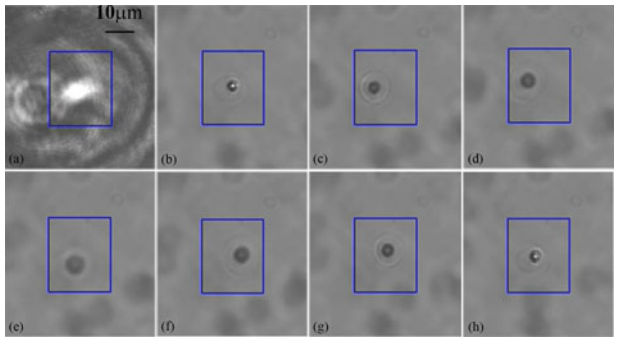

Fig. 7. Experimental demonstration of dynamic trapping with the second subsidiary foci of the fractional FZPs with N = 3, 3.001, 3.002, and 3.003, as well as S = 3, respectively. (a) The second subsidiary focus of the FZP with N = 3 and S = 3 and (b) the trapped microparticle in the viewfield of the CCD camera. (c)–(e) Trapped particle becomes blurred with dynamic changing of the fractional FZPs with N increasing from 3.001 to 3.003. (f)–(h) Trapped particle becomes clear again with N decreasing from 3.002 to 3.

further shifted upward synchronously until the second subsidiary focus approached the focal plane of the objective. In the process the polystyrene bead marked as 2 was attracted to the subsidiary focus and finally trapped stably at the focal plane of the objective. The trappings of the bead marked as 2 are shown in Fig. 6(d)–(f). In the experiments the polystyrene beads marked as 1 moved toward the bottom of the sample cell with the main focus and meanwhile the bead marked as 2 was trapped by the second subsidiary focus as is shown in Fig. 6(b)–(f). The results demonstrate that the particles can be trapped by the multiple foci of the fractional FZP beam in different planes simultaneously. Hence, when the FZPs are designed with a fractional number of fractal segments, the focal lengths of the foci can be finely tailored and customized trapping locations of trapped particles in 3-D space can be realized experimentally.

In fact, N can be modified with a variation as small as 0.001. For example, the main focus of the fractional FZP with N = 3.001 and S = 3 has shifting displacements of 0.2 mm in free space and 8 μm in the sample cell from that of the FZP with N = 3 and S = 3, respectively. Similarly, the corresponding subsidiary foci also have smaller shifting displacements. For comparisons, N can be modified with an increment of 1, e.g., from N = 2 to N = 3. The main focus of the FZP with N = 2 and S = 3 has shifting displacements of 804.9 mm in free space and 32.2 mm in the sample cell from that of the FZP with N = 3 and S = 3, respectively. Thus, microparticles can be dynamically manipulated by modifying N with an especially small fractional variation. For convenience we used the second subsidiary foci of the fractional FZPs to trap microparticles dynamically. Fig. 7(a) and (b) show the second subsidiary focus of the FZP with N = 3 and S = 3 and the trapped microparticle in the viewfield of the CCD camera, respectively. Then, the FZPs with N = 3.001, 3.002, and 3.003 were loaded on the SLM sequentially every 5 seconds. When N was increased, the second subsidiary focus of the corresponding fractional FZP was shifted toward the bottom of the sample cell. The experimental results are shown in Fig. 7(c)–(e), where the trapped particle becomes blurred with dynamic changing of the fractional FZPs in the SLM. Then, the FZPs with N = 3.002, 3.001, and 3.0 were loaded on the SLM sequentially every 5 seconds. The second subsidiary focus of the corresponding fractional FZP would be shifted toward the top of the sample cell. The dynamic trappings are shown in Fig. 7(f)–(h), where the trapped microparticle moves toward the original location and is in focus. Thus, the positions of the trapped particles can be dynamically controlled.

4. Conclusion

The axial properties of the optical beam generated by a fractional FZP were analytically investigated in this paper. The results demonstrated that the focal length of multiple foci of a fractional FZP

beam can be controlled precisely. The fractional FZP beam was first used in optical trapping and manipulating. In the trapping experiments the main focus and the second subsidiary focus of the fractional FZP beam with N = 2.9 and S = 3 were used to trap polystyrene beads. The experimental results demonstrated that the foci can manipulate particles stably and independently and even trap different microparticles in the two respective focal planes simultaneously. The results verify that the fractional FZP beam can be employed to construct 3-D optical tweezers where the trapping locations can be finely arranged.

References

[1] A. Ashkin, J. M. Dziedzic, J. E. Bjorkholm, and S. Chu, "Observation of a single-beam gradient force optical trap for dielectric particles," *Opt. Lett.*, vol. 11, no. 5, pp. 288–290, May 1986.

[2] S. B. Cheng, S. H. Tao, C. H. Zhou, and L. Wu, "Optical trapping of a dielectric-covered metallic microsphere," *J. Opt.*, vol. 17, Sep. 2015, Art. no. 105613.

[3] V. Bormuth *et al.*, "Optical trapping of coated microspheres," *Opt. Exp.*, vol. 16, no. 18, pp. 13831–13833, Sep. 2008.

[4] H. Melville and G. F. Milne, "Optical trapping of three-dimensional structures using dynamic holograms," *Opt. Exp.*, vol. 11, no. 26, pp. 3562–3567, Dec. 2003.

[5] J. Leach, G. Sinclair, P. Jordan, J. Courtial, and M. J. Padgett, "3-D manipulation of particles into crystal structures using holographic optical tweezers," *Opt. Exp.*, vol. 12, no. 1, pp. 220–226, Jan. 2004.

[6] A. Rohrbach and E. H. K. Stelzer, "Three-dimensional position detection of optically trapped dielectric particles," *J. Appl. Phys.*, vol. 91, no. 8, pp. 5474–5488, Apr. 2002.

[7] Z. Bouchal, J. Wagner, and M. Chlup, "Self-reconstruction of a distorted nondiffracting beam," *Opt. Commun.*, vol. 151, no. 4/6, pp. 207–211, Jun. 1998.

[8] J. Broky, G. A. Siviloglou, A. Dogariu, and D. N. Christodoulides, "Self-healing properties of optical Airy beams," *Opt. Exp.*, vol. 16, no. 17, pp. 12880–12891, Aug. 2008.

[9] V. Garces-Chavez, D. McGloin, H. Melville, W. Sibbett, and K. Dholakia, "Simultaneous micromanipulation in multiple planes using a self-reconstructing light beam," *Nature*, vol. 419, pp. 145–147, Sep. 2002.

[10] Z. Zheng, B. F. Zhang, H.Chen, J. P. Ding, and H. T. Wang, "Optical trapping with focused Airy beams," *Appl. Opt.*, vol. 50, no. 1, pp. 43–49, Jan. 2011.

[11] G. Saavedra, W. D. Furlan, and J. A. Monsoriu, "Fractal zone plates," *Opt. Lett.*, vol. 28, no. 12, pp. 971–973, Jun. 2003.

[12] S. H. Tao, B. C. Yang, H. Xia, and W. X. Yu, "Tailorable three-dimensional distribution of laser foci based on customized fractal zone plates," *Laser Phys. Lett.*, vol. 10, Feb. 2013, Art. no. 035003.

[13] J. X. Pu and P. H. Jones, "Devil's lens optical tweezers," *Opt. Express*, vol. 23, no. 7, pp. 8190–8199, Apr. 2015.

[14] W. D. Furlan, G. Saavedra, and J. A. Monsoriu, "White-light imaging with fractal zone plates," *Opt. Lett.*, vol. 2, no. 15, pp. 2109–2111, Aug. 2007.

[15] J. A. Monsoriu, W. D. Furlan, G. Saavedra, and F. Giménez, "Devil's lenses," *Opt. Exp.*, vol. 15, no. 21, pp. 13858–13864, Oct. 2007.

[16] D. Wu, L. G. Niu, Q. D. Chen, R. Wang, and H. B. Sun, "High efficiency multilevel phase-type fractal zone plates," *Opt. Lett.*, vol. 33, no. 24, pp. 2913–2915, Dec. 2008.

[17] V. Ferrando, F. Giménez, W. D. Furlan, and J. A. Monsoriu, "Bifractal focusing and imaging properties of Thue–Morse zone plates," *Opt. Exp.*, vol. 23, no. 15, pp. 19846–19853, Jul. 2015.

[18] J. A. Monsoriu, A. Calatayud, L. Remón, W. D. Furlan, G. Saavedra, and P. Andrés, "Bifocal Fibonacci diffractive lenses," *IEEE Photon. J.*, vol. 5, no. 3, Jun. 2013, Art no. 3400106.

[19] W. Z. Ma, S. H. Tao, and S. B. Cheng, "Composite Thue-Morse zone plates," *Opt. Exp.*, vol. 24, no. 12, pp. 12740–12747, Jun. 2016.

[20] S. H. Tao, X. C. Yuan, J. Lin, and R. E. Burge, "Sequence of focused optical vortices generated by a spiral fractal zone plate," *Appl. Phys. Lett.*, vol. 89, Jul. 2006, Art. no. 031105.

[21] S. B. Cheng, X. Y. Zhang, W. Z. Ma, and S. H. Tao, "Fractal zone plate beam based optical tweezers," *Sci. Rep.*, vol. 6, Sep. 2016, Art. no. 34492.